Available online at www.sciencedirect.com
SCIENCE DIRECT®
International Journal of Heat and Fluid Flow 25 (2004) 767–775
International Journal of HEAT AND FLUID FLOW
www.elsevier.com/locate/ijhff

# Comparative study of turbulent mixing in jet in cross-flow configurations using LES

B. Wegner *, Y. Huai, A. Sadiki

*Department of Mechanical Engineering, Institute for Energy and Powerplant Technology, Darmstadt University of Technology, Petersenstr. 30, 64287 Darmstadt, Germany*

Received 16 January 2004; accepted 6 May 2004
Available online 7 July 2004

**Abstract**

Mixing processes in turbulent fluid motion are of fundamental interest in many situations in engineering practice. Due to its practical importance in a vast number of applications, the generic configuration of the jet in cross-flow has been studied extensively in the past. Recently, the question has received a lot of attention, whether the unsteady behavior of the jet in cross-flow can be influenced by either active or passive means in order to control and enhance the mixing process. In the present paper, we use the large eddy simulation (LES) methodology to investigate how turbulent mixing can be enhanced by varying the angle between the jet and the oncoming cross-flow. After validating the computations against measurements by Andreopoulos and Rodi, we analyze qualitatively and quantitatively the mixing process for three configurations with different angles. It is shown that the inclination influences the characteristics of vortical structures and secondary motion which in turn have an effect on the mixing process. Besides a PDF of the passive scalar and a scalar energy spectrum, a mixedness parameter is used to provide information with respect to the quality and rate of mixing.


*Keywords:* Turbulent mixing; Large eddy simulation; Jet in cross-flow; Mixing enhancement

## 1. Introduction

Mixing processes in turbulent fluid motion are of fundamental importance in many situations in engineering practice such as pollutant formation, heat and mass transfer and chemical reactions. In a variety of engineering applications, the need for the efficiency of mixing systems and optimization of mixing processes has strongly increased. For example, a very important parameter in the design of lean premixed gas turbines is the degree of mixing between air and fuel prior to combustion. However, the physics of mixing processes are extremely complex and not well understood due to the intriguingly complex topology of the fluid and scalar motion. For complex configurations, a comprehensive knowledge of the phenomena can nowadays well be achieved by solving the equations governing the processes involved.

Due to its practical relevance in engineering and environmental applications, the generic configuration of the jet in cross-flow (in which a jet issues into a uniform free stream, boundary layer, duct flow, etc.) has been studied extensively in the past. A good review on the jet in cross-flow has been given by Margason (1993), hence we here restrict ourselves. Experimental data on turbulence and mixing statistics have been reported by a number of groups, e.g. Kelso et al. (1996) or Kim et al. (1999). In this paper, we chose the comprehensive measurements by Andreopoulos (1983) and Andreopoulos and Rodi (1984) as a reference to validate our simulations. During the last decade, many experimental as well as numerical studies have shown that the presence of three-dimensional and unsteady vortical structures provides a very efficient mechanism for the mixing process between the jet and the cross-flow. The complex vortical structures in the near field and the wake of the jet have been investigated by a number of groups. Using

* Corresponding author. Tel.: +49-6151-16-2357; fax: +49-6151-16-6555.
*E-mail address:* bwegner@ekt.tu-darmstadt.de (B. Wegner).

0142-727X/$ - see front matter © 2004 Elsevier Inc. All rights reserved.
doi:10.1016/j.ijheatfluidflow.2004.05.015

flow visualization techniques, Fric and Roshko (1994) found four different types of vortices. In addition to a horse-shoe vortex developing in front of the jet, the jet itself forms ring-like vortices (due to shear-layer instabilities) and a counter rotating bound vortex pair. Depending on the jet to cross-flow velocity ratio, wake vortices extending vertically from the wall to the jet can also be observed (similar to the wake vortices forming behind a bluff body). The mechanisms governing the development of these vortices are still a matter of debate as can be seen in Lim et al. (2001).

From a numerical point of view, the strongly unsteady behavior mentioned above makes steady-state modeling (i.e. Reynolds-averaged Navier–Stokes), at best, an approximation, suggesting the use of the large eddy simulation (LES) approach. By filtering the governing equations, all scales of motion and mixing smaller than a given filter width (the so-called sub-grid scales, SGS) are removed, while the large scales are explicitly computed. The influence of the unresolved small scales on the resolved flow must be modeled. Since the small scales of the flow are expected to be of universal nature, a high level of accuracy can be achieved in the prediction of flow by using relatively simple sub-grid models. For the scalar field, conclusive experimental evidence shows that structure functions and derivative skewness of the scalar field do not follow the assumption of isotropy at inertial and dissipative scales in the presence of a mean scalar gradient (see e.g. Warhaft, 2000 or Kang and Meneveau, 2001). This implies a direct effect of large-scale structures on small-scale structures, so that the anisotropic behavior of the micromixing has to be accounted for a consistent SGS scalar modeling (see Huai et al., in press). However, most simulations use an eddy diffusivity model in which the unresolved scalar flux terms are aligned with the resolved-scale scalar gradient and are assumed to be proportional to an isotropic sub-grid viscosity. This kind of models has found to give acceptable results in the past.

Early LES computations of a jet in cross-flow have been performed by Jones and Wille (1996). Yuan and Street (1998) used large eddy simulation to study the entrainment of cross-flow fluid into the jet which is important for the mixing process. Yuan et al. (1999) applied LES to investigate the effect of coherent structures upon the evolution of mean velocities, resolved Reynolds stresses, and turbulent kinetic energy along the center line of a round jet in cross-flow. Recently, results for LES of jets in cross-flow and its application to gas turbine burners were reported by Schlüter and Schönfeld (2000). Mengler et al. (2001) compared LES predictions of momentum and scalar fields with experiments by Andreopoulos and Rodi (1984) and Andreopoulos (1983) and second order turbulence closure calculations.

Lately, much attention has been paid to the question whether the unsteady behavior of the jet in cross-flow can be influenced by either active or passive means in order to control and enhance the mixing process. On the experimental side, Chang and Vakili (1995) introduced a periodic forcing of the jet to increase the mixing efficiency, Nakabe et al. (2001) investigated the influence of different arrangements of two jets inclined normal to the cross-flow direction and Wu et al. (2003) used a sleeve tube to influence the wall heat transfer for cooling jets. On the numerical side, Hilgers (2000) reported LES studies which aim at the improvement of the turbulent jet mixing. Prière et al. (2004) used large eddy simulation to study the effect of mixing devices on a row of jets issuing into a duct. However, no systematic study of the influence of geometrical parameters on the efficiency of the mixing has been numerically performed.

The present work focuses on a comparative analysis of the effect of an inclination of the jet with respect to the cross-flow direction on the flow and mixing phenomena using LES. We investigate three cases with a velocity ratio of $R = 0.5$ at a Reynolds number of 20,500: a jet issuing perpendicular into the cross-stream and two cases where the jets are inclined by +/−30°, respectively. We validate the obtained results with experimental data for the mean and turbulent flow and scalar quantities and analyze the configurations with respect to mean and turbulent statistics as well as the quality of mixing.

In Section 2, the governing equations are briefly presented along with the LES methodology and the numerical scheme. Section 3 specifies the configurations under investigation as well as the grid and boundary conditions used. Results are then reported in Section 4 in two steps. First, the precision of the LES results is evaluated by a comparison with available experimental data by Andreopoulos (1983) and Andreopoulos and Rodi (1984). Then, a comparative analysis of the mixing for the three cases is presented, emphasizing the influence of the unsteady vortical structures using appropriate quantitative parameters. Finally, our findings are summarized in Section 5.

## 2. Governing equations and numerical scheme

The filtered Navier–Stokes equations along with the filtered continuity equation describe the behavior of any Newtonian fluid here considered with constant density.

$$\frac{\partial \bar{u}_i}{\partial x_i} = 0, \tag{1}$$

$$\frac{\partial \varrho \bar{u}_i}{\partial t} + \frac{\partial}{\partial x_j}(\varrho \bar{u}_i \bar{u}_j) = \frac{\partial}{\partial x_j} \varrho \left( \nu \left( \frac{\partial \bar{u}_i}{\partial x_j} + \frac{\partial \bar{u}_j}{\partial x_i} \right) - \tau_{ij}^{\mathrm{SGS}} \right) - \frac{\partial \bar{p}}{\partial x_i}. \tag{2}$$

An additional filtered scalar transport equation is used to describe the evolution of a passive scalar, namely the mixture fraction $f$.

$$\frac{\partial \varrho \bar{f}}{\partial t} + \frac{\partial}{\partial x_i}(\varrho \bar{u}_i \bar{f}) = \frac{\partial}{\partial x_i}\varrho\left(D\left(\frac{\partial \bar{f}}{\partial x_i}\right) - J_i^{\mathrm{SGS}}\right). \tag{3}$$

The mixture fraction which is commonly used for diffusion flame modeling can be viewed as a dimensionless fuel concentration. It is defined as $f = 0$ for pure oxidizer and $f = 1$ for pure fuel. It can be used for any two-feed system to describe the mixing ratio between the two different fluids. The diffusion coefficient of mixture fraction $D$ is linked to viscosity via the Schmidt number ($D = \nu/Sc$), for which a value $Sc = 0.7$ is assumed. This relates to gaseous mixing.

A simple Smagorinsky model is employed for the sub-grid scale stress-tensor $\tau_{ij}^{\mathrm{SGS}}$, with Lilly's formulation of Germano's dynamic procedure for the determination of the model coefficient (Lilly, 1992). For the SGS scalar flux $J_i^{\mathrm{SGS}}$, let us recall that recent experimental evidence show that the scalar field does not follow the assumption of universality and isotropy at inertial and dissipative scales in the presence of a mean scalar gradient. This implies a direct effect of large-scale structures on small-scale structures. Therefore, the LES approach based upon the small-scale universality and isotropy with an absence of strong coupling across disparate length scales (energy cascade) is acceptable for momentum transport, but not valid for the small-scale mixing due to the anisotropic behavior of the micromixing. However, most simulations use an eddy diffusivity model in which the unresolved scalar flux terms are aligned with the resolved-scale scalar gradient and are assumed to be proportional to an isotropic sub-grid viscosity. Although modeling issues (see discussion in Section 1) are currently being studied by Huai et al. (in press), in the present work we employ the eddy diffusivity model for the sub-grid scalar flux $J_i^{\mathrm{SGS}}$, assuming a constant Schmidt number relationship between the turbulent diffusion coefficient and the turbulent viscosity

$$J_i^{\mathrm{SGS}} = -\frac{\nu_t}{Sc_t}\frac{\partial \bar{f}}{\partial x_i}; \quad Sc_t = 0.7. \tag{4}$$

All the governing equations are integrated into the three-dimensional finite-volume CFD code *FASTEST-3D*. The code features geometry-flexible block-structured, boundary-fitted grids with collocated variable arrangement. Second-order central schemes taking into account the grid non-orthogonality by means of multilinear interpolation (Lehnhäuser and Schäfer, 2002) are used for spatial discretization except for the convective term in the scalar transport equation. Here, a flux-limiter with TVD (total variation diminishing) properties is employed to ensure bounded solutions for the mixture fraction. Pressure-velocity coupling is achieved via a SIMPLE similar procedure. As time integration scheme the second-order implicit Crank–Nicolson method is used. The resulting set of linear equations is solved iteratively using a SIP-solver. The code is parallelized based on domain decomposition using the *MPI* message passing library. For details on the method refer to Durst and Schäfer (1996).

For code verification purposes, an opposed jet configuration with Reynolds number $Re = 6650$ investigated in house by Geyer et al. (2002) was computed first which will not be described here (see Wegner et al., 2003).

## 3. Configuration, grid and boundary treatment

The most important parameter besides Reynolds number characterizing mixing in the configurations under investigation is the velocity ratio computed from the bulk velocities of the two fluid streams. This ratio determines the level of shear between the two streams and hence the rate of mixing and is defined as $R = U_{\mathrm{jet}}/U_{cf}$ (assuming $\varrho = \mathrm{const}$). The base configuration investigated in this work was chosen to resemble the setup of Andreopoulos (1983) with $R = 0.5$. The jet issues perpendicular from a $D = 50$ mm pipe with $U_{\mathrm{jet}} = 6.95$ m/s into a cross-stream approaching along a flat plate with $U_{cf} = 13.9$ m/s (Fig. 1). The corresponding Reynolds number based on the jet velocity and pipe diameter is 20,500.

An O-grid was used to model the pipe. The extensions of the computational domain along with the grid resolution are listed in Table 1. The total size of the grid was 430,000 cells. Although this number might seem quite low, the reader should keep in mind that we are investigating a case with momentum ratio $R = 0.5$. This means that the jet does not penetrate far into the cross-flow and hence we do not need a large number of points in the wall-normal direction to achieve a good resolution. For validation purposes, we will later show a comparison with results obtained for the same case, but on a refined grid with $2 \times 10^6$ cells which indicate that the number of cells used was sufficient.

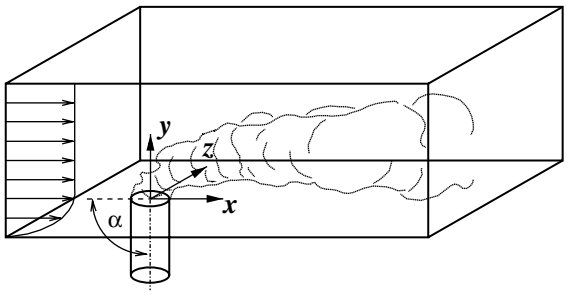


Fig. 1. Sketch of the problem domain along with the coordinate system employed.

Table 1
Size and numerical resolution of the computational domain

| | Direction | Length | Grid points |
|---|---|---|---|
| Cross-flow | Stream-wise | $x/D = -2, \ldots, 9$ | 128 |
| | Wall-normal | $y/D = 0, \ldots, 4$ | 54 |
| | Transverse | $z/D = -3, \ldots, 3$ | 52 |
| Pipe | Lengthwise | $y/D = -2, \ldots, 0$ | 40 |
| | O-block stream-wise | | 20 |
| | O-block transverse | | 16 |
| | O-block radial | | 10 |

In the two other cases, the jet pipe is inclined by 30° with and against the cross-flow direction. They are referred to as the 60°- and 120°-cases, respectively, with the inclination $\alpha$ as indicated in Fig. 1.

The inflow boundaries were treated as follows. For the jet pipe inflow artificial turbulence was generated based on DNS results for a pipe flow (Loulou et al. (1998)) employing the digital filtering method devised by Klein et al. (2003). For the cross-flow the same approach was tried first using DNS results from a plane boundary layer as input, but did not give satisfactory results. Hence, a fit to the experimental data was prescribed without any fluctuations which previously had given good results (Mengler et al., 2001). At the lateral boundaries a symmetry condition was applied and a Neumann condition was used for the outlet. On the solid walls a no-slip condition is applied with no special wall treatment for the SGS model. Instead, we rely on the ability of the dynamic procedure to capture the correct asymptotic behavior of the turbulent flow when approaching the wall (see e.g. Lesieur and Métais, 1996). This requires though that the boundary layer is resolved on the computational mesh which we have achieved by putting one grid point in the viscous sub-layer. Evaluation of the wall shear stress during the simulation indeed shows that the distance of the wall next point is $y^+ \approx 3$.

After the turbulent flow field had developed for all three cases, the simulations were run for some 20–30 flow through times (based on the cross-flow velocity) and statistics were sampled during this time. The time step size was chosen to get $\mathrm{CFL} \approx 1$.

## 4. Results and discussion

First, the results of the 90°-case are compared to the experimental data of Andreopoulos (1983) and Andreopoulos and Rodi (1984) to document the ability of the LES computations to precisely capture the flow and mixing phenomena in the investigated configuration. Then, the velocity and scalar fields of all three cases will be compared and the influence of the jet angle, especially on the mean and turbulent statistics as well as the global mixing quality, will be discussed.

### 4.1. Experimental Validation

Profiles in the jet center plane ($z/D = 0$) of mean velocities, turbulent kinetic energy as well as mean mixture fraction and its fluctuation are provided in Figs. 2–5. The computed mean axial and wall-normal velocities show a very good overall agreement with the experimental data. The existing deviations can be explained by the fact that the hot wire anemometry employed by Andreopoulos and Rodi (1984) is not able to determine the direction of the flow, an argument that has already been put forward by Schlüter and Schönfeld (2000). In contrast to the measurements, the LES shows a negative axial velocity at $x/D = -0.5$ which is linked to the well-known existence of a recirculation bubble upstream of the jet orifice. The same argument is applicable to the recirculation which is predicted by the LES at $x/D = 1$. Since the magnitude matches well and the neighboring positions are in good agreement with the experimental data it must be assumed that a recirculation exists here. This is actually supported by figure 1(a) in Andreopoulos and Rodi (1984) which is taken from an earlier paper by Foss (1980) and which clearly shows a recirculation.

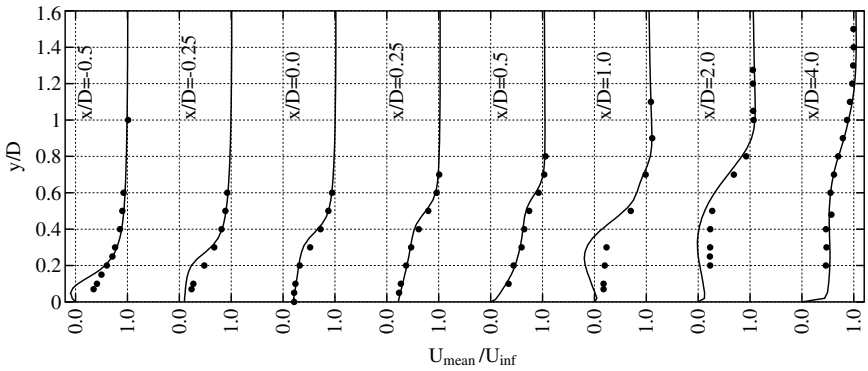


Fig. 2. Mean axial velocity for the 90°-case: LES (—), exp. data from Andreopoulos and Rodi (1984) (•).

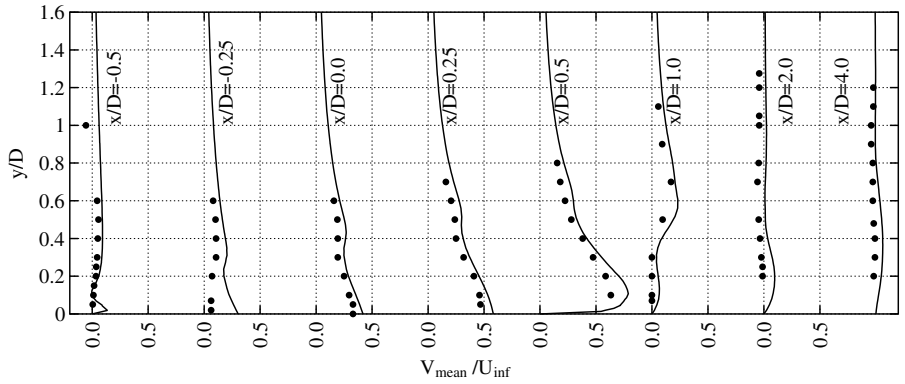


Fig. 3. Mean wall-normal velocity for the 90°-case: LES (—), exp. data from Andreopoulos and Rodi (1984) (●).

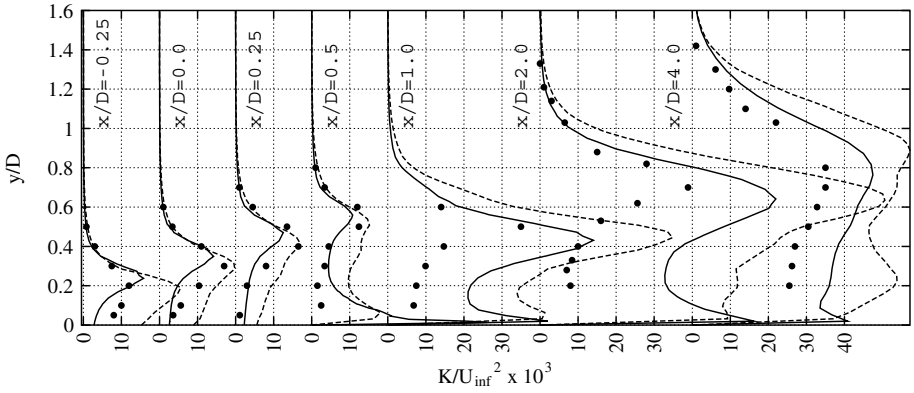


Fig. 4. Turbulent kinetic energy for the 90°-case: current LES (—), exp. data from Andreopoulos and Rodi (1984) (●). (- - -) LES from a refined grid ($2\times10^6$ cells).

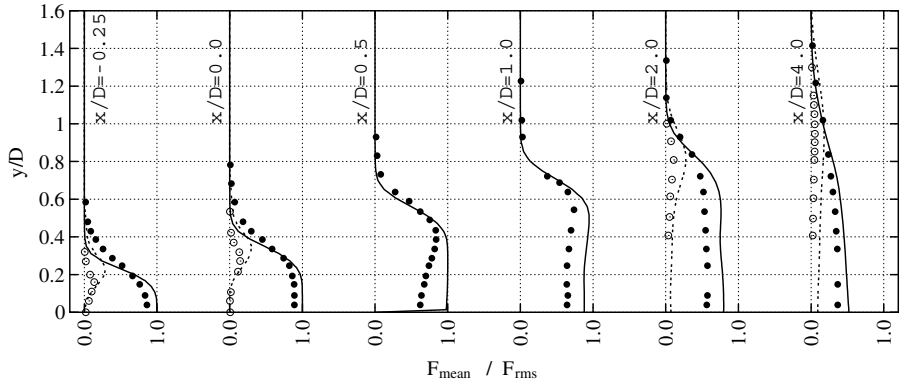


Fig. 5. Mixture fraction for the 90°-case: LES mean (—), exp. mean (●), LES RMS (- - -), exp. RMS (○). (Exp. data from Andreopoulos (1983)).

The turbulent kinetic energy $k$ (Fig. 4) shows good qualitative and quantitative agreement in the jet exit region, but in the region downstream of the jet exit, influenced by large-scale structures, the turbulent fluctuations seem to be over-predicted while the qualitative agreement is quite good. In their paper, Andreopoulos and Rodi (1984) specify the error for the velocity fluctuations as high as 10%. They also mention that the hot-wire anemometry employed for their measurements in general tends to underestimate turbulence quantities. [1] Differences between the LES and the work by Andreopoulos and Rodi (1984) might also arise from the fact that the experimental boundary conditions are not

[1] In conjunction with the fact that actual negative velocity samples were presumably recorded as positive by the hot-wire system used by Andreopoulos and Rodi (1984), the fluctuation as second moment of the PDF of velocity would be determined smaller than its real value.

documented very well and hence could not be matched in the simulation. This argument applies both to the oncoming cross-flow boundary layer and the pipe flow which in the simulation was assumed to be fully developed, but is surely influenced by the contraction nozzle employed in the experiments. In order to better judge in this matter, the quality of the LES was checked in several ways. First, the amount of resolved kinetic energy was estimated. To this end, the kinetic sub-grid energy $k^{\mathrm{SGS}}$ was computed according to Yoshizawa (1982) as

$$k^{\mathrm{SGS}} = \frac{v_t^2}{(C\Delta)^2}; \quad C = 0.086. \tag{5}$$

The grid resolution as the ratio of the resolved energy $k^{\mathrm{res}} = \frac{1}{2}\overline{u_i' u_i'}$ to the total energy contained in the flow,

$$G^{\mathrm{gs}} = \frac{k^{\mathrm{res}}}{k^{\mathrm{res}} + k^{\mathrm{SGS}}} \tag{6}$$

was found to exceed 80% in most parts of the jet with only a small region just behind the jet exit where the ratio was approximately 70%. These resulting values lie in the criteria range suggested by Pope (2000). Second, another simulation of the 90°-case was performed on a finer grid with a total of $2\times10^6$ cells to investigate the influence of the grid resolution. The results of this simulation are also plotted in Fig. 4. No big influence of the increased resolution on the profiles of the kinetic energy could be observed when comparing the results of the two simulations. We therefore believe that the differences between the simulation and the experiments are not due to an insufficient resolution.

Finally, the results obtained for the mixture fraction $f$ match quite well, too (Fig. 5). The position of the mixing layer and hence the penetration of the jet into the cross-stream agree precisely with the experimental data. For some reason which is not yet clear, the decay of mixture fraction inside the jet is slightly too slow. The RMS fluctuations of $f$ are reasonable when compared to the experiments. Overall, we think that the results well qualify LES to be used for the mixing analysis in the next section.

### 4.2. Mixing analysis

Mixing analysis is helpful in various practical fields in which control of mixing and flow is important (e.g. Hilgers, 2000; Prière et al., 2004). This can be achieved by capturing the influence of different parameters on the mixing rate. The latter can significantly be altered by varying the flow properties (Reynolds numbers, velocity ratios etc.), by imposing perturbations on the fluid flow or by modifying the geometry of the flow configuration.

In this section, we focus on the characterization of the mixing rate changes by varying the angle ($\alpha = 60°$, 90° and 120°) between the jet and the oncoming cross-flow (see Fig. 1). We now discuss the global mixing processes taking place in the three cases with different jet angles. We start by giving a qualitative description of the influence of the jet angle on the flow structures, entrainment mechanism and mixing process.

#### 4.2.1. Qualitative description

In Fig. 6, the time-averaged mixture fraction is shown at several axial positions for all three cases. It can be directly seen that the fluid coming from the jet is spread fastest in the 120°-case where the jet is injected against the cross-flow direction. Correspondingly, the mixing process is slowest in the 60°-case.

The question is now what physical factors are favorable for the enhanced mixing. The experimentally observed instabilities (Fric and Roshko, 1994) associated with the interactions between the jet and the cross-flow are related to the unsteadiness which occurs in both the bending of the jet by the cross-stream and the deflected streamlines of the mainstream. The entrainment into the jet and the resulting mixing process are then affected by various base vortex systems formed at the lee side of the jet, including a counter-rotating, kidney-shaped vortex pair, horse-shoe and Karman wake vortex on the wall. Flow animations for the different cases were created and it was noticed that an increased inclination of the jet results in an increased unsteady behavior of the jet. Fig. 7 gives (although showing just one instant of the flow) a good impression of this unsteadiness by looking at iso-surfaces of the $\lambda_2$-criterion. This criterion serves as a means to identify vortical structures (see e.g. Jeong and Hussain, 1995) and is defined as the second eigenvalue of the tensor

$$S_{ik}S_{kj} + \Omega_{ik}\Omega_{kj}, \tag{7}$$

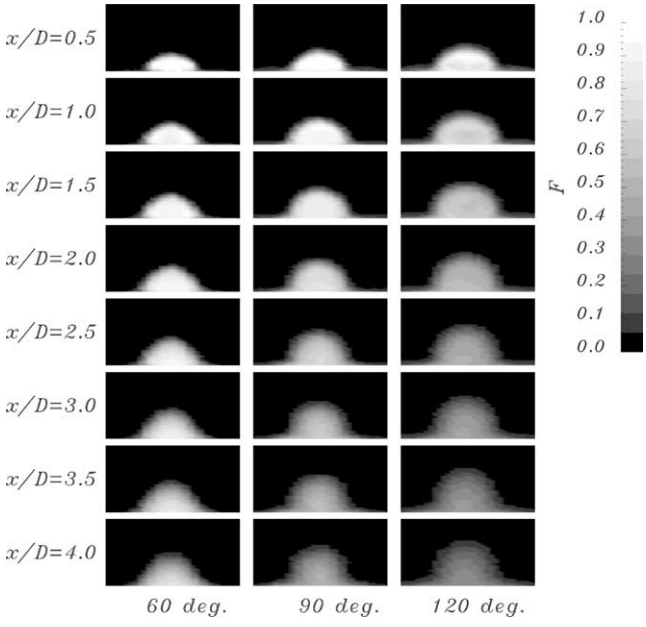


Fig. 6. Mean mixture fraction at several axial positions. Left: 60°-case, middle: 90°-case, right: 120°-case.

with $S_{ij}$ and $\Omega_{ij}$ being the symmetric and antisymmetric parts of the instantaneous velocity gradient tensor. Other vortex identification criteria such as the $Q$-criterion, the helicity and the magnitude of vorticity were also tried, but did not give as clear pictures as the $\lambda_2$-criterion. The horse-shoe, shear layer and counter-rotating vortices can clearly be identified in the pictures.

This increased amount of unsteadiness also results in more pronounced mean secondary flow features. As Fig. 8 shows, the strength of the counter-rotating vortex pair in the deflected jet increases for an increased inclination. This is due to the shear between the cross-flow and the jet exiting the pipe which first induces ring-like shear layer vortices which then develop into the pair of counter-rotating vortices in the jet (Yuan and Street, 1998). Since the shear is stronger when the jet is inclined towards the cross-flow, the vortices generated will also be stronger. This process also seems to increase the spreading rate of the jet. Since the cross-flow fluid is entrained into the jet by the secondary flow motion, the overall mixing rate is thus increased. In the following we will now discuss the mixing on a quantitative basis.

*4.2.2. Quantitative analysis*

After the qualitative description of the entrainment and mixing presented in the previous section we now aim at a quantitative analysis of the mixing process. In order to do this, two spatio-temporal quantities (the probability density function of the mixture fraction and the mixedness parameter) will be used besides the scalar energy spectrum. The influence of the jet angle on mixing can well be seen when looking at spatio-temporal probability density functions of the passive scalar. Fig. 9 shows such PDFs obtained by sampling instantaneous mixture fraction values in an axial plane at $x/D = 2$. All curves show a large portion of unmixed cross-flow fluid at $f = 0$ which simply comes from the fact that the samples were taken on an evenly spaced grid extending into the undisturbed cross-flow. Except from that, it can well be seen that both the shape and peak position of the distributions are influenced by the jet injection angle. While the 60°-case shows a bimodal shape with a narrow peak of rather unmixed jet fluid, the distributions of the two other cases are broader with the peak position being moved towards a mixed state with an increasing jet angle.

The spatial inhomogeneity of the scalar field is linked to the scalar fluctuation function as well as the corresponding scalar fluctuation dissipation function. Additional insight into the mixing behavior of the different configurations can therefore be gained by examining spectra of scalar energy. These are obtained by Fourier transformation of spatial autocorrelations of the scalar concentration and present a measure for the fluctuation of the scalar. The energy spectra shown in Fig. 10 were computed for the axial direction at the point $x/D = 4$, $y/D = 0.5$, $z/D = 0$. A number of experimental measurements of turbulent complex flows of practical importance have shown that the inertial sub-range with

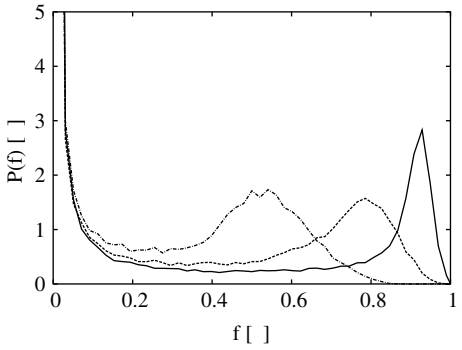


Fig. 9. Probability density function of mixture fraction in an axial plane $x/D = 2$. The three cases are denoted by: 60° (—), 90° (- - -) and 120° (-·-·-).

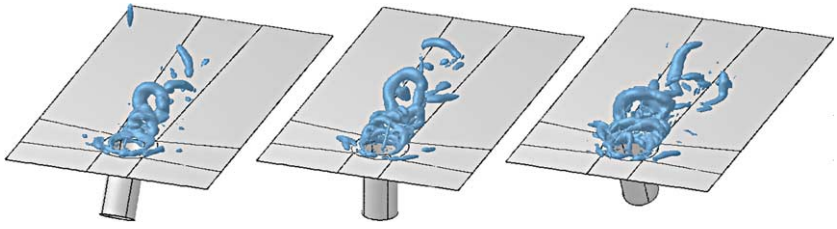

Fig. 7. Isosurfaces of the $\lambda_2$-criterion showing instantaneous vortex structures present in the three cases. Left: 60°-case; middle: 90°-case; right: 120°-case.

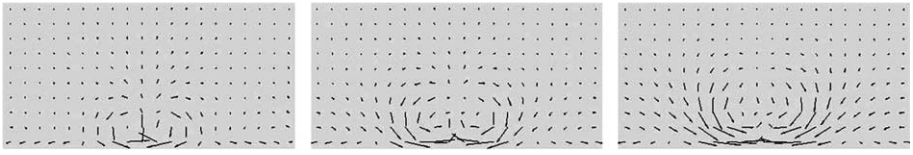

Fig. 8. Counter-rotating vortices in the secondary flow structure at $x/D = 2$. Left: 60°-case, middle: 90°-case, right: 120°-case.

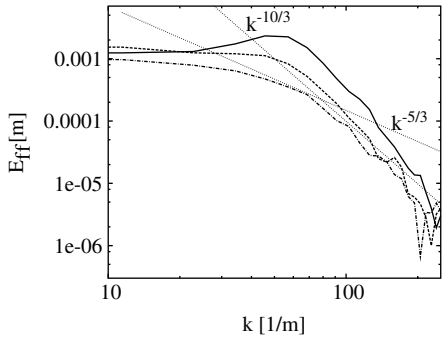


Fig. 10. Scalar energy spectrum computed from axial autocorrelations around $x/D = 4$. The three cases are denoted by: 60° (——), 90° (- - -) and 120° (-·-·-).

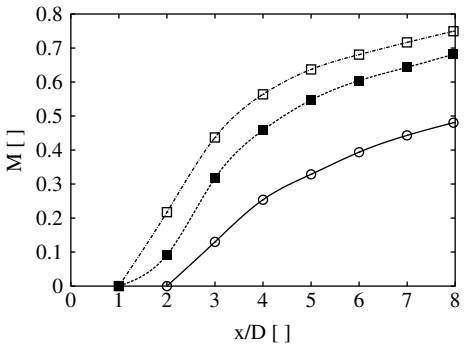


Fig. 11. Mixedness parameter for the three cases: 60° (○), 90° (■) and 120° (□).

−5/3 slope is often not so extended (see in Peng and Davidson, 2002) as in classical shear flows or jet flows (see in Kang and Meneveau, 2001). For complex flows with scalar transport, an additional sub-range exists next to the $k^{-5/3}$ sub-range with a steep dependence on $k$ according to $k^{-m}$, with generally $m > 5/3$. In Peng and Davidson (2002) $m = 3$ has been found. In Fig. 10, the spectrum exhibits a non-extended inertial range with a −5/3 slope followed at large wave numbers by a fairly clear sub-range with a −10/3 to −12/3 slope differing slightly for the three cases. It can now be seen that the level of scalar energy clearly differs for the three cases. While the 60°-case shows the highest level of fluctuations, the 90°- and 120° show consecutively lower fluctuation levels. Accordingly, in the 60°-case, mixing is most incomplete and in the 120°-case mixing has proceeded furthest. This backs up our above argumentation. Of course, if integrating the spectrum over all wave numbers, one gets the scalar variance $\overline{f'^2}$. Indeed, if plotting this quantity in a fashion similar to the plot of the mean mixture fraction in Fig. 6, one can see that the scalar fluctuations, although starting off at the jet exit with the highest values in the 120°-case, decay most rapidly in this case.

Up to now, the quantification of mixing by means of PDFs and scalar energy spectra has only been done on a local basis. We are interested in the global mixing, though. Various quantities have been introduced in the literature to account for a spatio-temporal quantification of the mixing (see Prière et al. (2004)), but the ability of these parameters to describe unequivocally the evolution of the mixing process is not clearly established. In this work, we choose a so-called "mixedness parameter" $M$ as proposed by Fric (1995).

$$M = 1 - \left[\int_A \int |(F - \bar{F})|\,\mathrm{d}A\right] \Big/ \left[\int_A \int |(F - \bar{F})|\,\mathrm{d}A\right]_0. \tag{8}$$

$F$ here denotes the time averaged mixture fraction. The integrals define the averaged deviation from the plane averaged mean $\bar{F}$ in planes perpendicular to the cross-flow. The index 0 in the denominator indicates that the deviation at some arbitrary position is normalized with the corresponding value at an initial position which in our case was set to the position of the peak value of the integral in the numerator of expression (8). The mixedness parameter $M$ lies within $[0, \ldots, 1]$ with 0 indicating completely separated fluids and 1 standing for completely mixed fluids.

In Fig. 11, the mixedness is plotted for all three cases. It can be seen that the growth rate (the slope of the mixedness parameter curve) of mixedness is almost the same for the 90°- and 120°-cases with the 90°-case lagging behind by approximately one jet diameter. The 60°-case shows a significantly smaller rate of mixing than the two other cases. For example, a value of $M = 0.5$ is hardly reached at $x/D = 8$ for the 60°-case, whereas the same degree of mixing is reached at $x/D = 3$ already for the 120°-case. It must be mentioned though, that the increase in mixing is accompanied by an increased pressure drop of ≈9% in the 120°-case compared to the perpendicular configuration.

## 5. Conclusions

We have once more demonstrated the ability of LES to precisely capture the flow and mixing features in jets in cross-flows when compared to experimental data. After validating our computations against available measurements, we performed simulations varying the angle between the jet and the cross-flow. It could be shown that this angle influences the characteristics of secondary flow features which in turn have an effect on the mixing process. In addition to PDFs of the scalar concentration or scalar energy spectra as presented above, the mixedness parameter provides valuable information about the rate and level of mixing in the different configurations.

All the parameters used lead to the same observation with regard to the evolution of the mixing rate in the

three cases investigated. From an engineering point of view it seems favorable to inject the jet at an angle inclined against the oncoming main flow. The increased mixing could help build shorter, lighter and cheaper devices.

## Acknowledgements

The authors gratefully acknowledge financial support by the *Deutsche Forschungsgemeinschaft* for funding through the Schwerpunktprogramm 1141 *"Analyse, Modellbildung und Berechnung von Strömungsmischern mit und ohne chemische Reaktionen"*.

## References

Andreopoulos, J., 1983. Heat transfer measurements in a heated jet-pipe flow issuing into a cold cross stream. Phys. Fluids 26 (11), 3201–3210.

Andreopoulos, J., Rodi, W., 1984. Experimental investigation of jets in a crossflow. J. Fluid Mech. 138, 93–127.

Chang, Y., Vakili, A., 1995. Dynamics of vortex rings in crossflow. Phys. Fluids 7 (7), 1583–1597.

Durst, F., Schäfer, M., 1996. A parallel blockstructured multigrid method for the prediction of incompressible flow. Int. J. Numer. Meth. Fluids 22, 549–565.

Foss, J., 1980. Interaction region phenomena for the jet in a cross-flow problem. In: Report SFB 80/E/161. Univ. Karlsruhe.

Fric, T., 1995. Skewed shear layer mixing within a duct. In: Proceedings of the 33rd Aerospace Sciences Meeting and Exhibit. AIAA 95-0869.

Fric, T., Roshko, A., 1994. Vortical structure in the wake of a transverse jet. J. Fluid Mech. 279, 1–47.

Geyer, D., Omar, S., Nauert, A., Ludwig, A., Dreizler, A., Janicka, J., 2002. A comprehensive characterization of a turbulent opposed jet flame by 1D-Raman/Rayleigh, 2D-LIF and LDV. In: Proceedings of the 1st International Workshop on Trends in Numerical and Physical Modelling For Turbulent Processes in Gas Turbine Combustors.

Hilgers, A., 2000. Direct simulation of a jet diffusion flame. Annual Research Briefs, Center for Turbulence Research.

Huai, Y., Wegner, B., Sadiki, A., in press. Effects of flow and scalar subgrid scale modelling on LES performance for mixing analysis. In: Proceedings of the 10th EUROMECH European Turbulence Conference, Trondheim, Norway, July 2004, to appear.

Jeong, J., Hussain, F., 1995. On the identification of a vortex. J. Fluid Mech. 285, 69–94.

Jones, W., Wille, M., 1996. Large eddy simulation of a round jet in a crossflow. In: Rodi, W., Bergeles, G. (Eds.), Engineering Turbulence Modelling and Measurements 3, Vol. 1. Elsevier, pp. 199–208.

Kang, H., Meneveau, C., 2001. Passive scalar anisotropy in a heated turbulent wake: new observations and implications for LES. J. Fluid Mech. 442, 161–170.

Kelso, R., Lim, T., Perry, A., 1996. An experimental study of round jets in cross-flow. J. Fluid Mech. 306, 111–144.

Kim, K., Kim, S., Yoon, S., 1999. PIV measurements of the flow and turbulent characteristics of a round jet in crossflow. In: The International Workshop on Particle Image Velocimetry, 16–18 September, Santa Barbara, CA, USA.

Klein, M., Sadiki, A., Janicka, J., 2003. A digital filter based generation of inflow data for spatially developing direct numerical or large eddy simulations. J. Comp. Phys. 186, 652–665.

Lehnhäuser, T., Schäfer, M., 2002. Improved linear interpolation practice for finite-volume schemes on complex grids. Int. J. Numer. Meth. Fluids 38, 625–645.

Lesieur, M., Métais, O., 1996. New trends in large eddy simulation of turbulence. Annu. Rev. Fluid Mech. 28, 45–82.

Lilly, D., 1992. A proposed modification of the Germano subgrid-scale closure method. Phys. Fluids 4 (3), 633–635.

Lim, T., New, T., Luo, S., 2001. On the development of large-scale structures of a jet normal to a cross flow. Phys. Fluids 13 (3), 770–775.

Loulou, P., Moser, R.D., Mansour, N., Cantwell, B., 1998. PCH00: Fully developed turbulent pipe flow simulations. In: A Collection of Test Cases for the Validation of Large Eddy Simulation. No. 345 in AGARD Advisory Reports. AGARD, Pipes and Channels (Chapter 5).

Margason, R., 1993. Fifty years of jet in cross flow research. In: AGARD-CP-534. AGARD, pp. 1.1–1.41.

Mengler, C., Heinrich, C., Sadiki, A., Janicka, J., 2001. Numerical prediction of momentum and scalar fields in a jet in cross flow: Comparison of LES and second order turbulence closure calculations. Turbulent Shear Flow Phenomena II 2, 425–431.

Nakabe, K., Fornalik, E., Eschenbacher, J., Yamamoto, Y., Ohta, T., Suzuki, K., 2001. Interactions of longitudinal vortices generated by twin inclined jets and enhancement of impingement heat transfer. Int. J. Heat Fluid Flow 22, 287–292.

Peng, S.-H., Davidson, L., 2002. On a subgrid-scale heat flux model for large-eddy simulation of turbulent thermal flow. Int. J. Heat Mass Transfer 45, 1393–1405.

Pope, S., 2000. Turbulent Flows. Cambridge University Press.

Prière, C., Gicquel, L., Kaufmann, P., Krebs, W., Poinsot, T., 2004. Large eddy simulation predictions of mixing enhancement for jets in cross-clows. J. Turbulence 5.

Schlüter, J., Schönfeld, T., 2000. LES of jets in cross flow and its application to a gas turbine burner. Flow, Turbulence Combustion 65, 177–203.

Warhaft, Z., 2000. Passive scalars in turbulent flows. Annu. Rev. Fluid Mech. 32, 203–240.

Wegner, B., Huai, Y., Sadiki, A., 2003. Analysis of the turbulent mixing in counterflow and jet in cross-flow configurations using LES. In: Hanjalić, K., Nagano, Y., Tummers, M. (Eds.), Turbulence, Heat and Mass Transfer 4. Begell House Inc, pp. 903–910.

Wu, H., Peng, X., Chen, T., 2003. Influence of sleeve tube on the flow and heat transfer behavior at a T-junction. Int. J. Heat Mass Transfer 46, 2637–2644.

Yoshizawa, A., 1982. A statistically derived subgrid model for the large-eddy simulation of turbulence. Phys. Fluids 25 (9), 1532–1538.

Yuan, L., Street, R., 1998. Trajectory and entrainment of a round jet in crossflow. Phys. Fluids 10 (9), 2323–2335.

Yuan, L., Street, R., Ferziger, J., 1999. Large-eddy simulations of a round jet in crossflow. J. Fluid Mech. 379, 71–104.